The Abdus Salam
International Centre for Theoretical Physics

United Nations
Educational, Scientific and
Cultural Organization

IAEA
International Atomic Energy Agency

2060-7

Advanced School on Non-linear Dynamics and Earthquake Prediction

28 September - 10 October, 2009

Spherical Block-and-Fault Model: Different Modification and Application to Simulation of Global Seismicity

V. L. Rozenberg / L. A. Melnikova
Institute of Mathematics and Mechanics
(1)Ural Branch of Russian Academy of Sciences
Ekaterinburg,
Russia

A. A. Soloviev
International Institute of Earthquake Prediction
Theory and Mathematical Geophysics
Moscow,
Russia

(1)www.imm.uran.ru/www.mitp.ru

Advanced School on Non-Linear Dynamics and Earthquake Prediction

28 September – 10 October 2009

Spherical Block-and-Fault Model: Different Modifications and Application to Simulation of Global Seismicity

V. L. Rozenberg (1), L. A. Melnikova (1), and A. A. Soloviev (2)

(1) Institute of Mathematics and Mechanics
Ural Branch of Russian Academy of Sciences
S. Kovalevskoi str. 16, Ekaterinburg 620219
Russian Federation
www.imm.uran.ru

(2) International Institute of Earthquake Prediction
Theory and Mathematical Geophysics
Russian Academy of Sciences
Profsoyuznaya str. 84/32, Moscow 117997
Russian Federation
www.mitp.ru

The Abdus Salam International Centre for Theoretical Physics, Strada Costiera 11, 34014 Trieste, Italy

2009

Abstract

The paper, being a continuation of the investigations [9, 10, 14, 15], where the approach to constructing the spherical block-and-fault model of lithosphere dynamics and seismicity is described, represents the review of developed modifications of the model and the discussion of their pros and cons. A comparative analysis of results of numerical experiments including synthetic earthquake catalogs, displacements of plates, and characteristics of their interaction along boundaries is performed. Actually, this paper should be treated as a revised and supplemented reedition of [15].

1 Introduction

Study of seismicity with the statistical and phenomenological analysis of real earthquake catalogs has the disadvantage that the reliable data cover, in general, a time interval of about one hundred years or less. This time interval is very short in comparison with the duration of tectonic processes responsible for the seismic activity. Therefore, the patterns of the earthquake occurrence identifiable in a real catalog may be only apparent and may not repeat in the future. In this connection, mathematical models of seismicity, i.e., of temporal-spatial earthquake sequences, are important tools that yield synthetic catalogs, which may cover a very long time interval that allows us to acquire more reliable estimates of parameters of a seismic flow and to search for premonitory patterns preceding large events [2]. Every event in a synthetic catalog is characterized by a time moment, epicenter coordinates, a depth, a magnitude, and, for some models, an intensity.

Let us note the principal features of the lithosphere as a complicated dissipative system that should be incorporated in a model for it to be regarded as adequate. First of all, this is the interaction of the processes of different physical origin and taking different spatial and temporal scales into account. Here, the fact is reflected that the two main mechanisms involved in the seismotectonic process, namely, the tectonic loading, with characteristic rate of a few cm/yr, and the elastic stress accumulation and redistribution, with characteristic rate of a few km/sec, should be considered in the typical time scale (10–100 yrs) as a uniform motion and an instantaneous stress drop, respectively. Further, this is the hierarchical block or possibly "fractal" structure of the lithosphere, and the universality of some its properties on both regional and global levels.

There exist many different approaches to modeling lithospheric processes (see [2] and its bibliography); nevertheless, we can mark out the two main directions. The first one is based on detailed investigation of a specific tectonic fault, or, rather often, a strong earthquake in order to reproduce certain pre- and/or post-seismic phenomena (relevant to this fault or event). In contrast, models of the second direction developed relatively recently treat the seismotectonic process in rather abstract way; the main goal of simulation is reproducing general universal properties of observed seismicity (primarily, the Gutenberg – Richter law on frequency-magnitude relation, clustering, migration of events, seismic cycle and so on). However, it seems that an adequate model designed in the framework of the second direction should reflect some universal features of nonlinear systems as well as the specific geometry of interacting tectonic faults. The block models of lithosphere dynamics and seismicity [1, 19] have been developed with both requirements taken into account. It should be noted that the problem of testing the model and comparing simulation results with real data is of independent interest.

In the block models, a seismically active region is represented as a system of rigid blocks that form a layer of a fixed thickness between two horizontal planes or concentric spheres. Lateral boundaries of the blocks consist of segments of infinitely thin faults. The system of blocks moves as a consequence of the prescribed motion of the boundary blocks and underlying medium. The displacement of a block may be described by three parameters (the two-dimensional model) as well as by six parameters (the three-dimensional model). The displacements of blocks at any time are defined so that the system is in a quasi-static equilibrium state. Because the blocks are perfectly rigid, all deformations take place in the fault zones and at the block bottoms. The interaction between the blocks is visco-elastic (a "normal state"), so long as the ratio of the stress to the pressure is below a certain strength level. When this level is exceeded in some part of a fault, a stress-drop (a "failure") occurs in accordance with the dry friction model. The failures represent earthquakes. Immediately following the earthquake for some period of time, the corresponding parts of the faults are in a "creep state". This state differs from the normal one because of the more rapid growth of inelastic displacements and continues until the stress falls below a given level. A synthetic earthquake catalog is produced as a main result of the numerical simulation. The information on displacements of blocks and their interaction along boundaries is also obtained.

The two-dimensional plane block model has been the most extensively studied. Models approximating dynamics of lithosphere blocks for real seismic regions have been built on its

basis [5, 12, 17, 19]. It has been used to study the dependence of properties of seismic flow on the geometry of faults and specific motions of the boundaries and underlying medium [7, 16, 19]. In the three-dimensional plane model [13], a vertical component of displacements has been taken into account introducing three additional degrees of freedom. The spherical geometry [9, 14] has been involved after significant distortions were revealed, while trying to simulate the motion of a system of global tectonic plates with plane block models. It is evident that the spherical modification is applicable to studying namely the motion of a global system, since in the case of a specific seismic region, due to the relative smallness of its dimensions, the influence of sphericity of the surface is negligible.

In the present paper, being a continuation of the investigations [9, 10, 14, 15], the emphasis is on the review of developed variants of the spherical model and on the discussion of their pros and cons. In the first variant, the so called "modification without depth" [9], it is assumed that all characteristics of a point are determined only by its coordinates and do not depend on the depth. The "modification with constant depth" used in [14] exploits the suggestion on the homogeneity of the lithosphere with respect to its depth and the identity of the depths of all blocks as well as of properties of all parts of a block (a fault). At last, the "modification with varying depth" introduced in [10, 15] represents an attempt of taking into account the inhomogeneity of the lithosphere by means of specification of different depths for different blocks and realization of an opportunity of changing fault properties depending on the depth.

2 Description of the model

Let us describe the basic constructions and ideas of the spherical block-and-fault model of lithosphere dynamics and seismicity.

2.1 Block structure geometry, block motion

A spherical layer of a depth H bounded by two concentric spheres is considered. The outer sphere represents the Earth's surface and the inner one represents the boundary between the lithosphere and the mantle. *A block structure* is a limited and simply connected part of this layer (see Fig. 1).

Partition of the structure into blocks is defined by *faults* intersecting the layer. Each

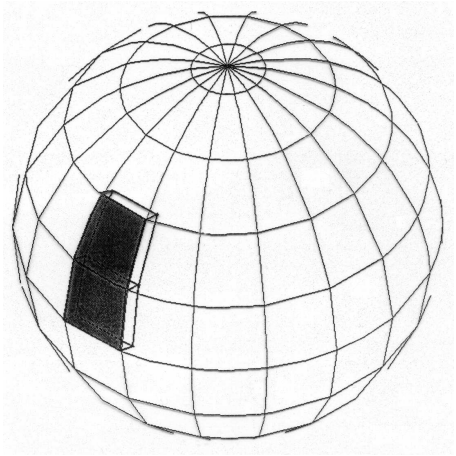

Figure 1: A model block structure on the sphere.

fault is a part of a cone surface characterized by the following two properties. Firstly, the intersection of the fault with the outer sphere (a fault line) is an arc of a great circle; the direction is specified for the fault line. Secondly, the vertex of the cone lies on the straight line, which is perpendicular to the great circle plane and passes through the center of the sphere. For such a definition of a fault, its *dip angle* with the outer sphere has the same value at all points of the fault line. We denote the dip angle (measured to the left of the fault line) as α. Thus, the geometry of a block structure is described by a system of fault lines on the outer sphere enclosing the layer, and by dip angles. Faults intersect along curves, which meet the outer and inner spheres at points called *vertices*. A part of such a curve between two respective vertices is called *a rib*. Fragments of faults limited by two adjacent ribs are called *segments*. The common parts of blocks with the limiting spheres are spherical polygons, those on the inner sphere are called *bottoms*. A block structure may be a part of the spherical shell and be bordered by *boundary blocks*, which are adjacent to boundary segments. Another possibility is to consider the structure including the whole spherical shell (covering the whole surface of the Earth) without boundary blocks. It should be noted that the possibility of considering a closed structure is a peculiarity of the spherical model (in comparison with plane modifications).

The blocks are assumed to be perfectly rigid. All block displacements are considered as negligible, compared with block sizes. Therefore, the geometry of the block structure does not change during the simulation, and the structure does not move as a whole. The gravitation forces remain essentially unchanged by the block displacements and, because the block structure is in a quasi-static equilibrium state at the initial time moment, gravity does

not cause a motion of the blocks.

All vertices on the outer sphere are defined by geographic coordinates (the latitude φ and the longitude ψ) in a spherical coordinate system with origin at the Earth's center (both this system and corresponding Cartesian system are called "System-O", Fig. 2).

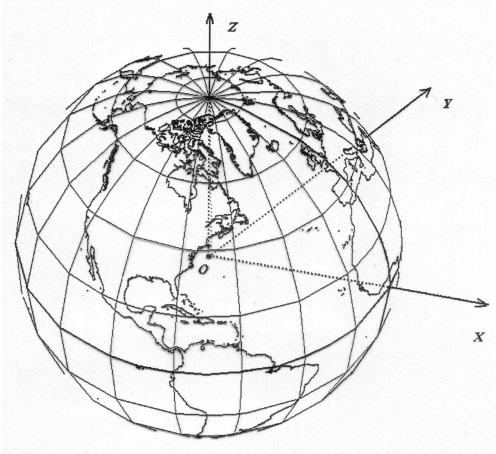

Figure 2: System-O.

In the spherical model, all blocks (both internal and boundary (if specified)) have six degrees of freedom and can leave the spherical surface. The displacement of each block consists of translation and rotation components. The translation component is determined by a translation vector (x, y, z). The rotation component is described by means of three angles γ, β, λ with respect to an immovable Cartesian coordinate system, (X, Y, Z), with the origin at the mass center of the block, point C with coordinates (φ_C, ψ_C, R_C). The X axis is directed along the parallel (latitude), the Y axis along the meridian (longitude), the Z axis is in the direction of the Earth's radius vector outwards. Denote this "System-C" (see Fig. 3).

Assume that the coordinate system with axes X_1, Y_1, Z_1 is connected to the mass center of the block (it coincides, in the absence of block displacements, with the immovable system of axes X, Y, Z, in which we consider all block motions). Rotation of the block and its corresponding system (X_1, Y_1, Z_1) with respect to the system (X, Y, Z) is given in Fig. 4. The first angle, γ, is defined as the angle of rotation of axes Y and Z around axis X such that if axis Z_2 is the intersection of planes XOZ_1 and YOZ, then axis Z is mapped into axis Z_2 and Y into Y_2. The second angle, β, is defined as the angle of rotation of axes X and Z_2 around axis Y_2 providing transformation of axis Z_2 into axis Z_1 (Z_1 is in the plane of XOZ_2) and X into X_2. And the third angle, λ, is defined as the angle of rotation of axes

X_2 and Y_2 around axis Z_1 such that X_2 and Y_2 transform into X_1 and Y_1, respectively.

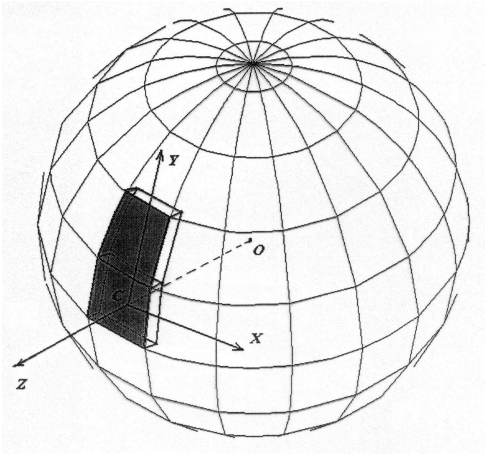

Figure 3: System-C.

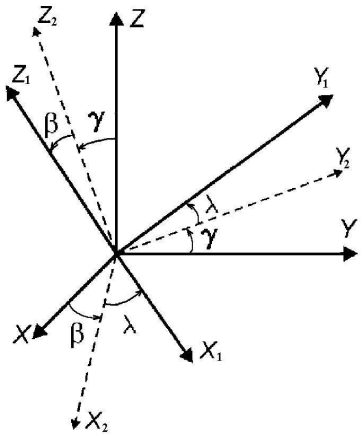

Figure 4: Definition of rotation angles γ, β, and λ.

According to the definition of the rotation angles, the displacement $(\Delta_x,\ \Delta_y,\ \Delta_z)$ at a block point with spherical coordinates $(\varphi,\ \psi,\ r)$ has the following form in System-C:

$$\Delta_x = x - \hat{Y}\lambda + \hat{Z}\beta, \quad \Delta_y = y + \hat{X}\lambda - \hat{Z}\gamma, \quad \Delta_z = z - \hat{X}\beta + \hat{Y}\gamma, \tag{1}$$

where $(x,\ y,\ z)$ is a block shift, $(\hat{X},\ \hat{Y},\ \hat{Z})$ are coordinates in System-C of the vector which is directed from the mass center of the block to the point $(\varphi,\ \psi,\ r)$, the angles $(\gamma,\ \beta,\ \lambda)$ are assumed to be small.

2.2 Visco-elastic interaction between blocks, equilibrium equations

The translation vector and the angles of rotation are found from the condition that the sum of all forces acting on the block, and the total moment of these forces, are equal to zero (the structure is assumed to be in a quasi-static equilibrium state). The forces arise on the inner sphere due to relative displacements of the blocks with respect to the underlying medium and on the fault surfaces due to displacements of neighboring blocks. The motions of the boundary blocks (if they are specified) and of the underlying medium, considered as an external action on the structure, are assumed to be known. As a rule, they are described as rotations on the sphere, i.e., axes of rotation and angular velocities (Euler vectors) are given. Another possibility consists in specifying a field of velocities (by some law or point-wise) for points belonging to the boundary blocks and/or the underlying medium.

Depending on the way of treating the depth of the spherical layer, several modifications of the model are worked out. Since this depth is significantly less than the linear dimensions of a block structure, it seems reasonable to consider only points belonging to a fault line on the Earth's surface while computing the properties of block interaction. Thus, it is assumed that all characteristics are described only by coordinates (φ, ψ) and do not depend on r. This version of the model is called the "modification without depth". Its main advantage consists in considerable saving of running time during simulations; it may be essential in the case of a large number of runs for carrying out an experiment with the variation of some parameters. The cons are obvious: a) actually, dip angles are not properly taken into account; b) studying the mechanism of spreading an earthquake along a fault is impossible; c) the range of changing the model magnitude is significantly narrowed. That is why the second modification (the "modification with depth", more complicated but more adequate) is designed. At that, two versions are developed, namely, a) with the same depth of the spherical layer for a whole structure (the "modification with constant depth") and b) with a possibility of specifying different depths for different blocks and of changing fault parameters depending on its depth (the "modification with varying depth"). Below, presenting some constructions, which are general for all the modifications, we dwell on the specificity of each modification.

Consider a point on the outer sphere with coordinates (φ, ψ) belonging to some fault separating blocks with numbers i and j, with block i on the left, and block j on the right

(the depths of these blocks may be different). Denote by $\vec{e}_t$ the unit vector tangent to the fault line at this point and directed along the fault. Let it have coordinates $\vec{e}_t = (e_1, e_2, 0)$ in the rectangular coordinate system with origin at the point (φ, ψ) and axes introduced analogously to those of system-C (call it "system-P"). Define the vector $\vec{e}_l = (-e_2 \cos\alpha, e_1 \cos\alpha, -\sin\alpha)$, which lies on the plane tangent to the fault's surface at the given point and is perpendicular to the vector $\vec{e}_t$ (α is a dip angle of the fault and, consequently, of the tangent plane). Introduce also the vector $\vec{e}_n = (-e_2 \sin\alpha, e_1 \sin\alpha, \cos\alpha)$ that is perpendicular to this plane. Let the righthanded triple $(\vec{e}_t, \vec{e}_l, \vec{e}_n)$ define the rectangular coordinate system with the origin at the point (φ, ψ), "system-T", see Fig. 5.

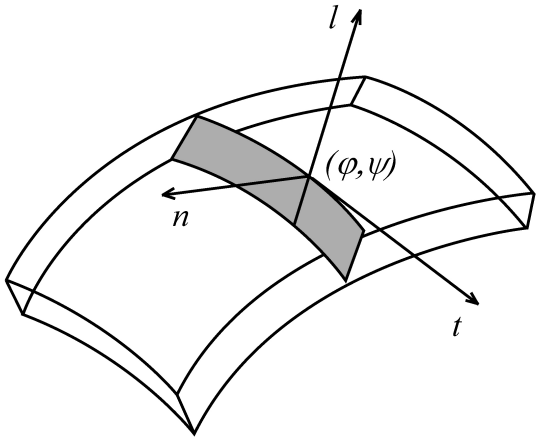

Figure 5: System-T.

Note that, in the modifications with depth, it is assumed that system-P and system-T described above are used for all points of the fault "corresponding" to the point on the outer sphere with the coordinates (φ, ψ). It turns out that, by means of two introduced coordinate systems, one can rather easily write out relations for finding displacements and elastic forces.

Now consider an arbitrary point (φ, ψ, r) of the fault mentioned above, see Fig. 6. Let (Δ_x^{rel}, Δ_y^{rel}, Δ_z^{rel}) be the vector of relative displacement of the blocks (or the block and the underlying medium of the neighboring block) at the point (φ, ψ, r) in system-P. Components of displacement on the plane tangent to fault's surface at this point and in the direction that is perpendicular to this plane (i.e., in system-T) are correlated with Δ_x^{rel}, Δ_y^{rel}, Δ_z^{rel} as follows:

$$\Delta_t = \Delta_x^{rel} e_1 + \Delta_y^{rel} e_2, \quad \Delta_l = -\Delta_x^{rel} e_2 \cos\alpha + \Delta_y^{rel} e_1 \cos\alpha - \Delta_z^{rel} \sin\alpha,$$

$$\Delta_n = -\Delta_x^{rel} e_2 \sin\alpha + \Delta_y^{rel} e_1 \sin\alpha + \Delta_z^{rel} \cos\alpha.$$

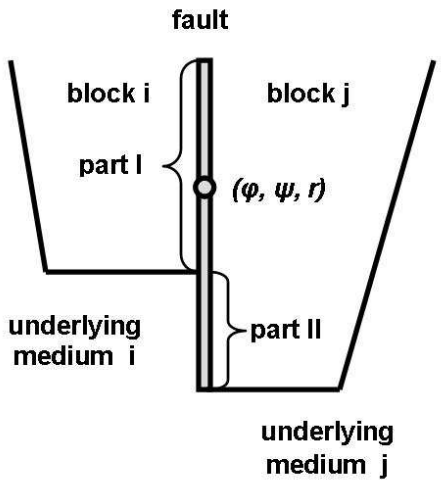

Figure 6: Peculiarity of a fault separating blocks of different depths.

The elastic force per unit area (f_t, f_l, f_n) applied to the point (φ, ψ, r) of the fault is defined by

$$f_t = K_t(\Delta_t - \delta_t), \quad f_l = K_l(\Delta_l - \delta_l), \quad f_n = K_n(\Delta_n - \delta_n). \tag{2}$$

Here δ_t, δ_l, δ_n are corresponding inelastic displacements, the evolution of which is described by the equations

$$\frac{d\delta_t}{dt} = W_t f_t, \quad \frac{d\delta_l}{dt} = W_l f_l, \quad \frac{d\delta_n}{dt} = W_n f_n. \tag{3}$$

The coefficients K_t, K_l, K_n, W_t, W_l, and W_n in (2) and (3) may be different for different faults and, in addition, may depend on the depth (in the modification with varying depth). The values K_t, K_l, and K_n are considered as the shear modulus in the corresponding directions, whereas the values W_t, W_l, and W_n are inverse to the viscosities [5, 19].

Now, calculate the components of relative displacement, Δ_x^{rel}, Δ_y^{rel}, and Δ_z^{rel}, with the use of formulae (1). We obtain

$$\Delta_x^{rel} = \Delta_x^i - \Delta_x^j, \quad \Delta_y^{rel} = \Delta_y^i - \Delta_y^j, \quad \Delta_z^{rel} = \Delta_z^i - \Delta_z^j, \tag{4}$$

where (Δ_x^i, Δ_y^i, Δ_z^i) and (Δ_x^j, Δ_y^j, Δ_z^j) are vectors of displacement (in system-P) of the point (φ, ψ, r) respectively as a point of the blocks i and j (in the case when the point belongs to part I of the fault, see Fig. 6) or as a point of the underlying medium of the block i and the block j (in the case when the point belongs to part II of the fault, see Fig. 6).

In order to obtain the components of these vectors, one should multiply the displacements in systems-C (defined by (1)) of the point (φ, ψ, r) as a point of of the blocks i and j (or of

the underlying medium) by the transformation matrix from system-C corresponding to the block (or to the underlying medium) to system-P (these formulae are omitted here due to their length). Let us note only that in this way one can determine the displacements both for points on any fault and on the block bottom.

In system-P (associated with a point (φ, ψ) of the block bottom) the elastic force per unit area, (f_x^u, f_y^u, f_z^u), is of the form:

$$f_x^u = K_u(\Delta_x^u - \delta_x^u), \quad f_y^u = K_u(\Delta_y^u - \delta_y^u), \quad f_z^u = K_u^n \Delta_z^u, \tag{5}$$

where δ_x^u, δ_y^u are the corresponding inelastic displacements, the evolution of which is given by the equations:

$$\frac{d\delta_x^u}{dt} = W_u f_x^u, \quad \frac{d\delta_y^u}{dt} = W_u f_y^u. \tag{6}$$

It is assumed that there is no any inelastic displacement in the vertical direction (along axis z of system-P). The coefficients K_u, K_u^n, and W_u in (5) and (6) may be different for different blocks. The vector $(\Delta_x^u, \Delta_y^u, \Delta_z^u)$ of relative displacement of the block and the underlying medium at the point (φ, ψ) considered in system-P is defined by (1) and (4) analogous to the case of finding the displacement at a fault point.

As mentioned above, components of the translation vectors of the blocks, and angles of their rotation around the mass centers of the blocks, are found from the condition that the total force and the total moment of forces acting on each block (written in system-C corresponding to the block) are equal to zero. This is the condition of quasi-static equilibrium of the system, and at the same time the condition of energy minimum.

It is important that the dependence of forces and moments on displacements and rotations of blocks is linear. Therefore, the system of equations for determining these values must be linear:

$$\mathbf{A}\mathbf{w} = \mathbf{b}. \tag{7}$$

Here, the components of the unknown vector $\mathbf{w} = (w_1, w_2, ..., w_{6n})$ are components of translation vectors of blocks and angles of their rotation (n is the number of blocks), i.e., $w_{6m-5} = x_m$, $w_{6m-4} = y_m$, $w_{6m-3} = z_m$, $w_{6m-2} = \gamma_m$, $w_{6m-1} = \beta_m$, $w_{6m} = \lambda_m$ ($m = 1, 2, ..., n$). The elements of matrix $\mathbf{A}$ ($6n \times 6n$) and of vector $\mathbf{b}$ ($6n$) are determined from rather complicated formulae, which are deduced from (1)–(6) with the transformation of forces and moments to system-C. For brevity sake, these formulae are omitted here. It should be noted that the matrix $\mathbf{A}$ in (7) does not depend on time and its elements are

calculated only once, at the beginning of the process. The components of vector $\mathbf{b}$ depend on time, explicitly, because of motions of the underlying medium and boundary blocks and, implicitly, because of inelastic displacements.

2.3 Discretization

The model uses dimensionless time. When interpreting the results, some realistic value should be given to one unit of dimensionless time. For computational purposes, the time discretization is performed by introducing a time step Δt. The state of the block structure under consideration is determined at discrete times $t_i = t_0 + i\Delta t$ $(i = 1, 2, \ldots)$, where t_0 is the initial time. The transformation from the state at t_i to the state at t_{i+1} is made as follows: a) new values of inelastic displacements δ_t, δ_l, δ_n, δ_x^u, δ_y^u are calculated from equations (3) and (6); b) translation vectors and rotation angles at t_{i+1} are calculated for the boundary blocks (if they are specified) and the underlying medium; c) components of $\mathbf{b}$ in system (7) are found, and this system is used to determine the translation vectors and rotation angles for the blocks.

To calculate various curvilinear integrals, one should discretize (divide into cells) the spherical surfaces of the block bottoms and fault segments. The values of forces and inelastic displacements are assumed to be equal for all points of a cell. The block bottoms are divided into cells in a natural way with the use of a longitude-latitude grid, see Fig. 7; steps with respect to longitude and latitude are specified, the former depends on the latter.

Note that, according to the assumption, in the modification without depth segments are not subject to any discretization by depth (while calculating, we use characteristics of cells belonging to fault lines on the Earth's surface). In the modifications with depth, a cone surface of a fault inclined under some angle α is approximated by a family of planes with the same inclination angle (Fig. 8). Steps of the discretization along and deep down segments are specified.

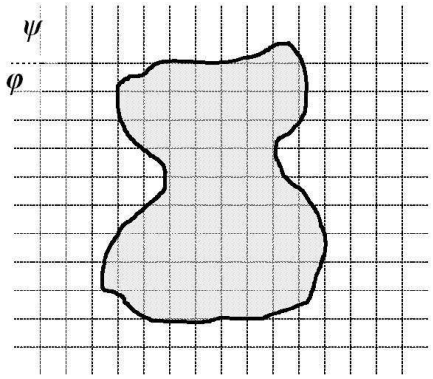

Figure 7: Discretization of a block bottom.

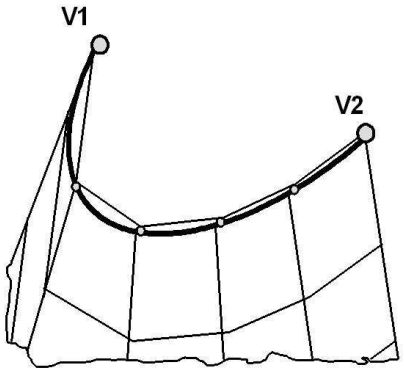

Figure 8: Discretization of a fault segment with vertices v1 and v2.

A good approximation of a cone surface by a family of planes in the case of a small enough partition along the fault line substantiates the usage of system-P and system-T described above for all points belonging to the layer (in depth) corresponding to the point of the outer sphere with coordinates (φ, ψ).

2.4 Earthquake and creep

For every time moment, we calculate the value of a quantity κ by the following formula

$$\kappa = \frac{\sqrt{f_t^2 + f_l^2}}{P - f_n}, \tag{8}$$

where P is the parameter, which may be interpreted as the difference between the lithostatic and the hydrostatic pressure (P has the same value for all faults).

For every fault, three levels of κ are specified. They satisfy the inequalities $B > H_f \geq H_s$. It is assumed that the initial conditions for numerical simulation of block structure dynamics

satisfy the inequality $\kappa < B$ for all cells of the fault segments. If, at some time t_i, the value of κ in some cell of a fault segment reaches level B, a failure ("earthquake") occurs. By a failure we mean a slippage by which the inelastic displacements δ_t, δ_l, δ_n in the cell change abruptly to reduce the value of κ to the level H_f. The new values of the inelastic displacements are calculated from

$$\delta_t^e = \delta_t + \gamma^e \xi_t f_t, \quad \delta_l^e = \delta_l + \gamma^e f_l, \quad \delta_n^e = \delta_n + \gamma^e \xi_n f_n, \tag{9}$$

where δ_t, δ_l, δ_n, f_t, f_l, f_n are the inelastic displacements and the components of the elastic force vector per unit area just before the failure. The coefficients $\xi_t = K_l/K_t$ ($\xi_t = 0$ if $K_t = 0$) and $\xi_n = K_l/K_n$ ($\xi_n = 0$ if $K_n = 0$) account for inhomogeneities of displacements along the plane tangent to the fault (in various directions), and normal to that plane (they account for the possibility that the same value of the elastic force per unit area can result in different changes of different inelastic displacements). The coefficient γ^e is given by

$$\gamma^e = \frac{\sqrt{f_t^2 + f_l^2} - H_f(P - f_n)}{K_l\sqrt{f_t^2 + f_l^2} + K_n H_f \xi_n f_n}. \tag{10}$$

It follows from (2) and (8) through (10) that after the calculation of new values of the inelastic displacements and elastic forces, the value of κ in the cell is equal to H_f. It should be noted that after the calculation according to (2) and (9), the signs of the elastic forces must be the same as just prior to the failure. For this reason, some cases, namely, a) $(1 - K_n\xi_n\gamma_e) < 0$ (and f_n changes the sign) and b) $(1 - K_l\gamma_e) < 0$ (and f_l, f_t change the signs; it is proved that this situation is possible only for $f_n < 0$) require additional processing. In both cases, we assume

$$\delta_n^e = \Delta_n, \quad \gamma^e = \frac{\sqrt{f_t^2 + f_l^2} - H_f P}{K_l\sqrt{f_t^2 + f_l^2}}.$$

Only then the new components of vector $\mathbf{b}$ are computed, and the translation vectors and angles of rotation for the blocks are found from (7). If for some cell(s) of the fault segments $\kappa \geq B$, the entire procedure is repeated. This is done until all cells satisfy the condition $\kappa < B$, at which point the state of the block structure at time t_{i+1} is determined as described in Section 2.3. Immediately after the earthquake, it is assumed that the cells, in which the failure occurred, are in the creep state. This implies that, for these cells, parameters W_t^s ($W_t^s > W_t$), W_l^s ($W_l^s > W_l$), and W_n^s ($W_n^s > W_n$) are used instead of W_t, W_l, and W_n in equations (3). Such new values provide the faster growth (comparing with the normal state) of the inelastic displacements. They may be different for different faults. The cells are in

the creep state so long as $\kappa > H_s$; when $\kappa \leq H_s$, the cells return to the normal state, after which W_t, W_l, and W_n are used in (3).

All cells of the same fault, in which the failure occurred at the same time, are considered as a single earthquake. The parameters of the earthquake are defined as follows: a) the time of the event is t_i; b) the epicentral coordinates are the weighted sums of the corresponding coordinates of the cells involved in the earthquake (the weight of each cell is given by its length (in the modification without depth) or area (in the modifications with depth) divided by the sum of lengths/areas of all cells involved in the earthquake); c) the magnitude is calculated in the modification without depth by the formula [21]:

$$M = 1.16 \lg L + 5.08, \tag{11}$$

where L is the total surface rupture length of cells (in km) involved in the earthquake (at that, it is possible to attribute the same depth to all earthquakes); and in the modifications with depth by the formula [20]:

$$M = 0.98 \lg S + 3.93, \tag{12}$$

where S is the total area of cells (in km^2) involved in the earthquake. In [21] one can find the updated relationship between the magnitude and rupture area with the new value of the absolute term in (12), which is equal to 4.07. Evidently, if we use the updated formula in the model, earthquakes magnitudes will be slightly higher. An argument to use formulae (11) and (12) as a definition of the model magnitude is the fact that the energy released through an earthquake depends mainly on the total size (area) of fault's part covered by this earthquake. Thus, a synthetic earthquake catalog is produced as a main simulation result.

3 Results of numerical experiments

To compare different modifications of the spherical block model, we consider results of numerical modeling of dynamics and seismicity of the global system of tectonic plates. This block structure is a closed one including the whole spherical shell (covering the whole surface of the Earth). It does not have lateral boundaries and therefore boundary blocks are not specified for it. Previous analysis [9] proved that dynamics and seismicity of the global system of tectonic plates is more accurately modeled by means of the closed block structure than with the structure for that boundary blocks (e.g., the largest plates) are specified.

Therefore, in this study we restrict ourselves by considering the closed system of plates only. The detailed description of numerical experiments with the modification without depth can be found in [14]. Due to this reason and the fact that now this modification is actually almost out of practice, here we give only the outline of corresponding simulation results.

3.1 Modification without depth

The block structure approximating the global system of tectonic plates includes 15 blocks, 186 vertices, and 199 faults (segments), see Fig. 9.

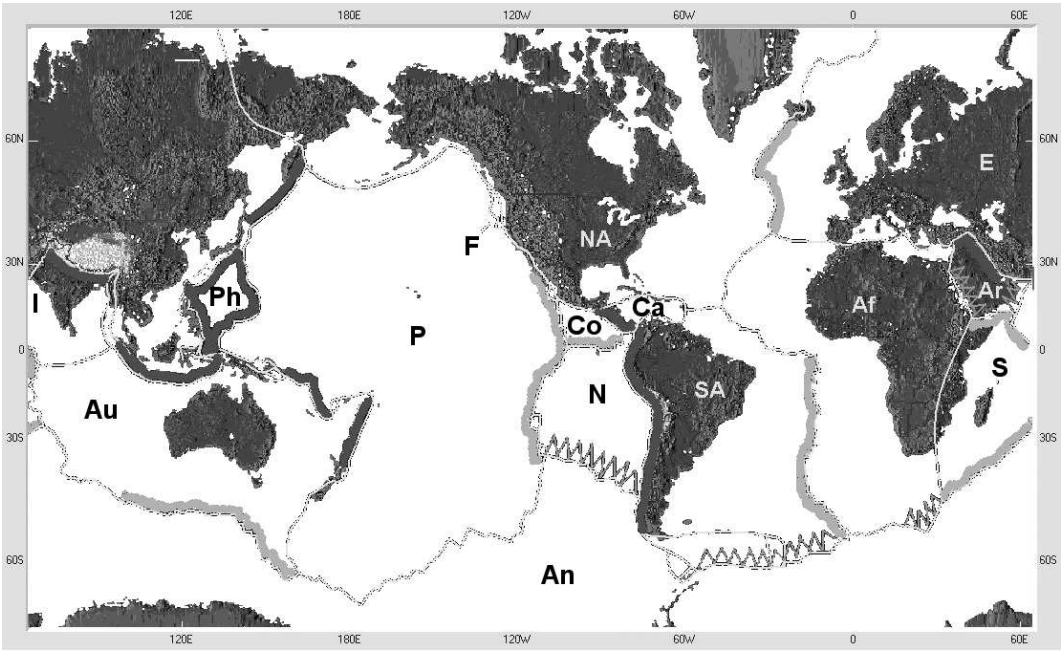

Figure 9: The global system of tectonic plates and results of simulation of the character of plate boundaries: divergent plate boundaries (spreading, light shading), convergent plate boundaries (subduction, dark shading), transform plate boundaries (sliding, toothed shading). The notation for the plates: NA — North America, SA — South America, N — Nazca, Af — Africa, Ca — Caribbean, Co — Cocos, P — Pacific, S — Somalia, Ar — Arabia, E — Eurasia, I — India, An — Antarctica, Au — Australia, Ph — Philippines, F — Juan de Fuca.

We use dip angles of faults to consider flat gradient of subduction zones in comparison with other plate boundaries. Thus we specify a dip angle of 50° for faults corresponding to clearly observed subduction zones (e.g., at the boundaries South America/Nazca, India/Eurasia, Cocos/Caribbean, around Philippines; totally 26 faults) and of 90° for other

faults. It is obvious that in the modification without depth a dip angle is rather artificial characteristic of a fault.

The motion of the closed structure is caused only by the motion of the underlying medium. The parameters of the latter are taken from the model HS2-NUVEL-1 [4] with the Somalia plate added [6]. The values of the coefficients in formulae (2), (3), (5), and (6) are specified using the experience of the previous studies with the plane block models (see, e.g., [17, 19]) and taking into account the peculiarities of the spherical block model. The coefficients K_t, K_l, K_n, K_u, K_u^n are measured in bar/cm, the coefficients W_t, W_l, W_n, W_u — in cm/bar. In all the experiments described below, if not mention otherwise, there are taken the following values of parameters determining the interaction between a block and its underlying medium (see (5),(6)): $K_u = 10, W_u = 0.1, K_u^n = 20$ and the following values for the levels of κ (see (8)): $B = 0.02, H_f = 0.017, H_s = 0.014$. Increasing slightly (comparing with the plane models) the values of the first group provides the better binding of blocks to their underlying medium (this corresponds to the common views on the plate tectonics), whereas decreasing the values of the second group is explained by the desire of getting larger number of model events on a bounded time interval.

Several series of numerical experiments studying the dependence of dynamics and seismicity of the structure on model parameters, in particular, on characteristics of visco-elastic properties of block bottoms and faults, are carried out. The changes of these parameters are based on observed seismicity: the coefficients K_t, K_l, K_n are decreased, and the coefficients W_t, W_l, W_n are increased for faults with vastly low level of observed seismicity (as a rule, for faults that separate large-scale structures); and vice versa for active faults. These changes reflect the following considerations [19]. First, if the same value of relative displacement of two blocks separating by a fault zone is considered then it induces a lesser force at a large-scale fault zone than at a small-scale one. This means that smaller values of coefficients K_t, K_l, K_n should correspond to large-scale fault zones. Second, the rate of growth of inelastic displacement for the same value of the force should be greater for large-scale fault zones, which are more fragmented, than fault zones separating small-scale structures. This means that larger values of coefficients W_t, W_l, W_n should correspond to large-scale fault zones. The experiments allowed us to specify a set of parameters which provided the better correspondence between model and real data. This set is presented in Tab. 1 (the notation for the plates is introduced in Fig. 9).

T a b l e 1

Parameters of basic variant

Parameters of discretization	Parameters of faults
Time step — 0.01. Space step: for segments — 1 km, for block bottoms — 0.5°.	For faults that form boundaries NA/SA, west of I/Au, E/NA: $K_t = K_l = K_n = 0.1$, $W_t = W_l = W_n = 1$; east of SA/An, south of SA/Af: $K_t = K_l = K_n = 0.25$, $W_t = W_l = W_n = 0.4$; west of SA/An, Co/N, P/N, An/N, Co/P, Af/NA, south of Au, west of F, south of P: $K_t = K_l = K_n = 0.5$, $W_t = W_l = W_n = 0.2$; SA/N, middle of SA/An, north of SA/Af, E/Ar, east of I/Au, I/E, north of Au, P/NA: $K_t = K_l = K_n = 2$, $W_t = W_l = W_n = 0.05$; around Ca, NA/Co, E/Af, east and north-east of Au, E/Au, around Ph: $K_t = K_l = K_n = 5$, $W_t = W_l = W_n = 0.02$. For other faults: $K_t = K_l = K_n = 1$, $W_t = W_l = W_n = 0.1$.

The results of numerical experiments include the spatial distribution of the strongest model events, the information on displacements of the plates and on the character of their interaction along boundaries. Below we present some simulation results for the variant from Tab. 1.

The behavior of boundary points belonging to plate boundaries, for which one of three types (divergent, convergent, and transform) is clearly marked, is investigated. Such characteristic boundaries [11] (e.g., as South America/Nazca, Pacific/Nazca, South America/Africa, India/Eurasia, surrounding Philippines, etc.) are considered. By means of two displacements of a boundary point in the coordinate system connected with this point (system-P) as a point of right and left blocks, respectively, its relative displacement is computed. Relative

displacements of boundary points characterize qualitatively the interaction between plates along their boundaries, namely, allow us to mark the divergent (spreading), convergent (subduction), and transform (sliding) plate boundaries; this information is partly presented in Fig. 9. The model boundary types are rather similar to real ones.

In addition, the spatial distribution of the strongest model events is obtained. The comparative analysis of the synthetic catalog that is composed by means of formula (11) and observed seismicity is performed. We consider events with the magnitude $M \geq 5.0$ for the time period 01.01.1900–31.12.2008 without any restrictions by depth and area of location selected from the global catalog NEIC [3] (below NEIC-5). Studying the spatial distribution of epicenters of the model events shows most active synthetic seismicity at such boundaries as Nazca/South America, Cocos/Caribbean, India/Eurasia, California region, Arabia/Eurasia, south-east, east, north-east and, especially, north of Australia, and the Philippine plate margin. The level of synthetic seismicity is extremely small at such boundaries as south of Pacific plate, Nazca/Pacific, east and south-west of Africa, India/Australia, North America/Eurasia. These locations agree in principle with observations; this fact indicates a degree of adequacy of the model. The similarity in the locations of epicenters of the strongest events in observed seismicity (Fig. 10) and model one (Fig. 11) is evident, despite of some differences (e.g., north of Africa, boundary South America/Africa). Note that the magnitudes in the spherical block model are, as a rule, larger than the real ones. At the same time, the analysis of parameters of the Gutenberg — Richter law, of vertical components of block motions in subduction zones, of some quantitative characteristics of motions brings to light not quite satisfactory results. In particular, the slope of the FM plot characterizing the relation between the numbers of strong and weak events is far from the real value, whereas the plot is far from linear (it is known that the FM plot for global seismicity observed during the period of last 100 years is nearly linear and its slope is approximately equal to 1). Thus, we made the conclusion that the model needs to be improved. As main directions of its development, we chose taking into account the depth of the spherical layer and the lithosphere inhomogeneity. The variant from Tab. 1 is considered as a basic one for testing the modifications with depth.

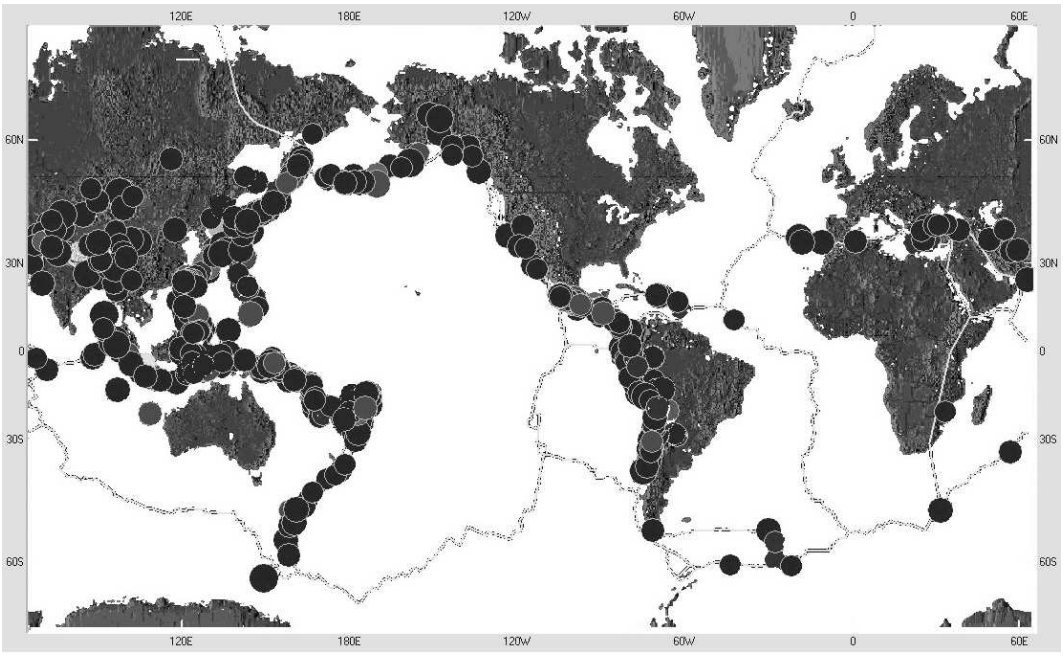

Figure 10: Epicenters of strongest earthquakes with $M \geq 7.5$, catalog NEIC-5.

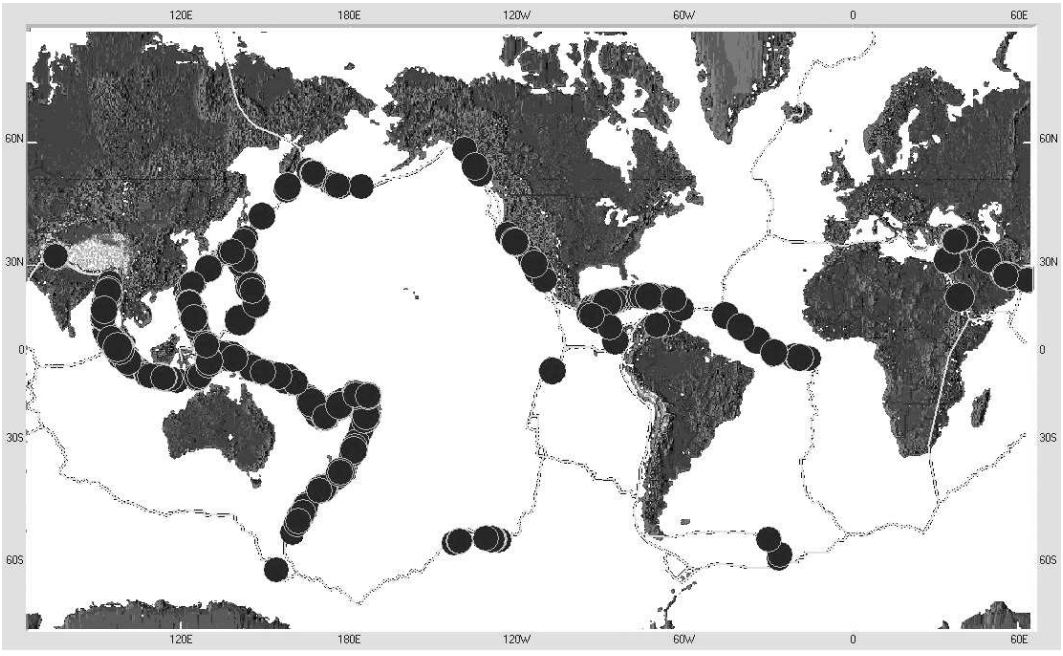

Figure 11: Epicenters of strongest earthquakes with $M \geq 8.0$, modification without depth, variant from Tab. 1.

3.2 Modification with constant depth

The simulation of dynamics of the block structure described in the previous section is performed on the base of the variant from Tab. 1. In this section, we assume that the depth of the spherical layer (the lithosphere in the model) is of the same value for all the blocks, namely 40 km. The parameters of faults listed in Tab. 1 remain unchanged during experiments.

Let us describe some simulation results. Three series of experiments are carried out. The first series (Tab. 2, variants 1.1–1.4) investigates the dependence of the Gutenberg — Richter law parameters for global seismicity, of the seismic flow intensity, and of the range of changing the model magnitude on the value of the step of discretizating segments by depth (all other parameters including dip angles (their influence on simulation results should essentially increase for the modification with depth) are the same). The second series (Tab. 2, variants 2.1–2.3) is designed to study the impact of faults' dip angles. Third one (Tab. 2, variants 3.1–3.4) repeats the first series but the best variant of the second series is chosen as a basic one. Again, as in the previous section, we orientate ourselves to the parameters of the Gutenberg — Richter law for observed seismicity. The characteristics of the interaction between plates along their boundaries and the spatial distribution of the strongest model events are similar in different variants and do not have principal distinctions from the results obtained by means of the modification without depth. The parameters being of interest are presented in Tab. 2. Note that the magnitude of model events in the modifications with depth is calculated by formula (12).

Analyzing the data from Tab. 2, we can point out the following facts. The simulation results obtained in variants 1.1–1.4 do not allow us to assert that there exists a definite dependence of the slope of the FM plot on the value of the step of discretizating segments by depth in the case when the majority of faults have got dip angles of 90°. Although the slope is slightly increased when the step is decreased (this is rather "good" tendency), the approximation error is also increased. Some extension of the range of changing the model magnitude takes place due to decreasing the minimal area of segment cells. In variants 1.1–1.4, the slopes of the model FM plots are less than 1. It is likely that the matter is in the fact that failures occur simultaneously in cells belonging to faults with dip angles of 90°. Therefore, strong events prevail over others, the FM plot is more gently sloping, and the influence of the step of the discretization by depth is vague.

T a b l e 2

Modification with constant depth: simulation results

Variant	Step of discretization	Number of model events	Range of changing magnitude	Slope estimate	Approximation error
1.1	40 km	237 389	[5.4,8.8]	0.804	0.232
1.2	20 km	282 305	[5.2,8.7]	0.848	0.274
1.3	8 km	328 400	[4.5,8.8]	0.876	0.236
1.4	4 km	344 984	[4.3,8.8]	0.886	0.296
2.1 = 1.3	8 km	328 400	[4.5,8.8]	0.876	0.236
2.2	8 km	340 401	[4.5,8.7]	0.883	0.230
2.3	8 km	419 120	[3.9,8.5]	0.841	0.154
3.1	40 km	324 385	[5.3,8.7]	0.828	0.177
3.2	20 km	376 240	[4.7,8.6]	0.844	0.186
3.3 = 2.3	8 km	419 120	[3.9,8.5]	0.841	0.154
3.4	4 km	436 619	[3.6,8.5]	0.845	0.162

Remarks.

1. All plots are approximated by the linear least-squares regression, $\lg N = a - bM$. A slope estimate for the plot is a "b-value" of corresponding regression. The average distance between points of the plot and the line constructed is treated as an approximation error.
2. In variants 2.2 and 2.3, dip angles being equal to 90° in the basic variant (Tab. 1) are substituted for 75° and 105° (depending on fault's direction) in such a way: for 26 faults adjacent to subduction zones in variant 2.2, and for almost all faults in variant 2.3 (angles being equal to 50° are not changed).
3. The interval of simulation is equal to 100 units of dimensionless time for all variants.
4. The magnitude interval for the plot is equal to $[5.5, 7.5]$ for all variants.

In variants 2.1–2.3, we observe the essential extension of the range of changing the model magnitude due to the occurrence of weak events and some "improvement" of the approximation error of the slope of the model FM plot. This happens chiefly because of cells of a fault with dip angle different from 90° come to "critical" state at different time instants; and, as a consequence, we have got a greater number of weak events.

According to the aggregated estimate, variant 2.3 should be recognized as a better one in the second series. Namely for this variant the value of the step of discretizating segments

by depth is varied in the third series (variants 3.1–3.4). It is easily seen that in this series, when decreasing the step, the essential (comparing with the first series) extension of the range of changing the model magnitude and some "improvement" of linearity of the model FM plot are observed (at that the slope is closest to 1 in variant 3.4). This fact points out an essential distinction in the properties of model seismicity in the cases when dip angles are equal to 90° and are not.

The analysis of the results obtained in three series leads to the conclusion that the shape of the model FM plot is to a greater degree determined by dip angles of faults in comparison with the value of the step of discretizating segments by depth. Indeed, decreasing of this value influences the intensity of the flow of model earthquakes but does not result in changes of the number of events in a magnitude interval common for all model catalogs. The total number of earthquakes increases due to the occurrence of weak events of lesser magnitudes defined by the minimal area of segment cells (see (12)); at that the slope is slightly varied. Fig. 12 confirms these conclusions.

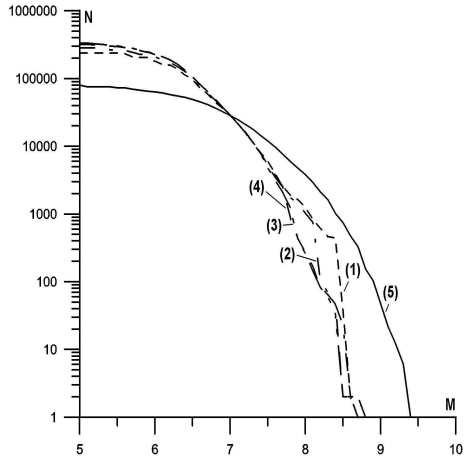

Figure 12: The model FM plots constructed for variants 1.1–1.4 (Tab. 2, (1)–(4), respectively) and for the variant obtained by the modification without depth (5); N is accumulated number of earthquakes, M is magnitude.

To compare with the data from Tab. 2, we use the results obtained by means of the modification without depth. For the variant from Tab. 1, the number of model events is equal to 79 694, the slope of the model plot on the magnitude interval [5.5,7.5] is equal to 0.372, the approximation error is 0.067.

One can see from Fig. 12 that plot (5) constructed for the variant obtained by the modification without depth is essentially less linear (as a whole) in comparison with others.

In this plot, one can identify two almost linear parts with different slopes; the intermediate zone between these parts is observed nearby magnitude point $M = 7.0$. Such bend of the shape of the FM plot may be explained as follows: it reflects transition from earthquakes involving whole "short" segments to earthquakes involving whole "long" segments. When taking into account the depth of the layer, such clear bend is not observed since cells obtained as a result of the spatial discretization by depth afford more uniform filling of the magnitude range for model events. In addition, according to plot (5), there are rather many events with abnormally large magnitudes in this variant. Such distinctions allow us to conclude that, at least, according to some characteristics, the modification with constant depth is more adequate in the description of global seismicity than the modification without depth.

To compare the model and real data, the FM plots for synthetic seismicity in variant 3.4 and that for observed seismicity constructed from catalog NEIC-5 are given in Fig. 13.

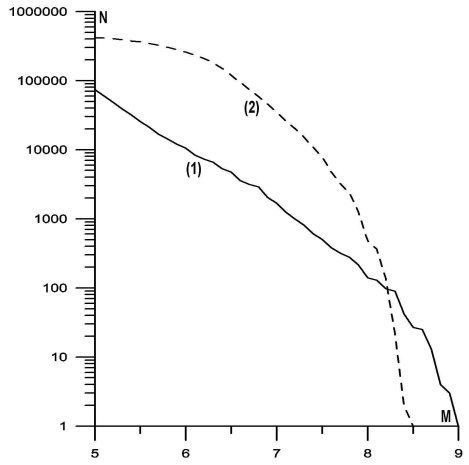

Figure 13: The FM plots constructed for the real (NEIC-5, (1)) and synthetic (variant 3.4, (2)) catalogs; N is accumulated number of earthquakes, M is magnitude.

For the model plot in Fig. 13, there exists the magnitude interval (the domain of average values), where the plot is "linear enough". But this plot essentially differs from the real one, especially outside the domain in question. To reduce differences, it is necessary to increase the number of weak events in the model and to improve "linearity" of model plots. Toward this end, additional series of numerical experiments in which different values of depth are assigned to different blocks and properties of faults are changed depending on depth (thus taking into account the lithosphere inhomogeneity) are carried out.

As to the spatial distribution of the strongest model events, it is slightly different in variant 3.4 (Fig. 14) from the distribution in the variant obtained by the modification without

depth (Fig. 11). As pros of variant 3.4, we consider the occurrence of strong events on the known by its seismic activity boundary South America/Nazca.

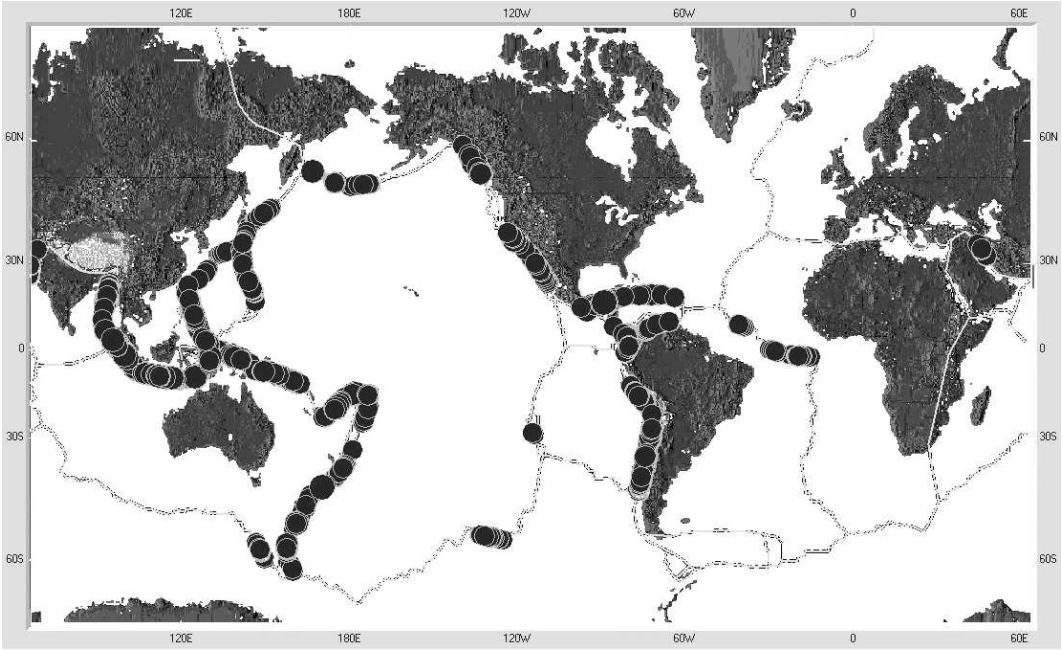

Figure 14: Epicenters of strongest earthquakes with $M \geq 7.0$, modification with constant depth, variant 3.4 from Tab. 2.

Note that in some regions, where rather high seismicity is observed, we did obtain strong earthquakes in all the variants (e.g., in the west part of boundary Africa/Eurasia, see Fig. 10). Our conjecture is that the motion of global tectonic plates is not a main driving force of seismic activity in these regions.

3.3 Modification with varying depth

During numerical experiments with the modification with varying depth described in this section, the model plate depths for the structure under consideration (see Fig. 9) are specified taking into account a) the distribution in depth of real earthquakes from catalog NEIC [3]; b) the fact that the depth of a block actually determines the range of changing the depth of model events on this block's boundaries (recall that, according to the model assumptions, events cannot occur inside a block). By this reasoning, the following depths are assigned to the blocks: Nazca — 50 km, South America — 10 km, Cocos — 50 km, Caribbean — 10 km, North America — 10 km, Pacific — 100 km, Africa — 10 km, Antarctica — 10 km,

Eurasia — 30 km, Arabia — 50 km, India — 50 km, Somalia — 10 km, Philippines — 50 km, Australia — 50 km, Juan de Fuca — 50 km. Note that, under such a specification, the depths of some blocks (e.g., of Pacific plate) essentially differ from commonly accepted estimates of real values [8]. The next step in the development of this modification is assumed to be a partition of the model plates into blocks with mainly continental (deep) crust and mainly oceanic (thin) crust. Such a restructuring will allow us to specify block depths in accordance with their real values; it is impossible in the present situation due to essential inhomogeneities of the blocks in the sense that the same block may contain considerable parts with the crust of different types (e.g., South and North American plates).

Two series of experiments are carried out. In the process, the step of discretizating segments by depth remained the same, namely 2 km. The first series (Tab. 3, variants 4.1–4.3) investigates the dependence of some properties of synthetic seismicity on the rule for changing the coefficients from (2) and (3) characterizing visco-elasticity of a fault medium with depth. Note that dynamics of coefficients is chosen in such a way that it provides the approximate equality of products K_tW_t, K_lW_l, and K_nW_n on each layer of the discretization of a segment by depth. This restriction is explained by the fact that the values that are inverse to listed products are important rheological characteristics of a fault [5]. In variant 4.1, all the coefficients mentioned above do not depend on depth; in variant 4.2, the coefficients K_t, K_l, and K_n are decreased with depth on the basis of 2% per every layer (e.g., for faults of Philippines from 5 bar/cm on the surface layer down to 3 bar/cm at a depth of 50 km), whereas the coefficients W_t, W_l, and W_n are increased by analogy (e.g., for faults of Philippines from 0.02 cm/bar on the surface layer up to 0.033 cm/bar at a depth of 50 km); in variant 4.3, vice versa, the coefficients K_t, K_l, and K_n are increased on the basis of 2% per every layer (for mentioned faults from 5 bar/cm up to 8.2 bar/cm), whereas the coefficients W_t, W_l, and W_n are decreased by analogy (for mentioned faults from 0.02 cm/bar down to 0.012 cm/bar). In the second series, the influence of other model parameters is studied. In variant 5.1, the parameters specifying the interaction between a block and its underlying medium are changed (see (5),(6)): $K_u = 1, W_u = 0.025, K_u^n = 2$ instead of $K_u = 10, W_u = 0.1, K_u^n = 20$. In variant 5.2, the coefficients W_t^s, W_l^s, and W_n^s used to calculate inelastic displacements of cells being in the creep state are multiplied by five (comparing with all other variants).

For a comparative analysis of simulation results, in addition, we involve variant 3.4 from Tab. 2 (as the best one in the modification with constant depth). Tab. 3 presented below is

composed by analogy with Tab. 2.

T a b l e 3

Modification with varying depth: simulation results

Variant	Number of model events	Range of changing magnitude	Slope estimate	Approximation error
3.4	436 619	[3.6,8.5]	0.845	0.162
4.1	506 175	[3.8,8.6]	1.844	0.650
4.2	598 087	[3.5,8.0]	—	—
4.3	831 151	[3.2,8.3]	—	—
5.1	457 558	[3.6,9.0]	1.690	0.349
5.2	404 599	[3.6,8.6]	1.827	0.150

Remarks.

1. The interval of simulation is equal to 100 units of dimensionless time for all variants.

2. The magnitude interval for the plot is equal to $[6.5, 8.0]$ in variants 4.1, 5.1, and 5.2; $[5.5, 7.5]$ in variant 3.4; intervals of linearity are uncertain in variants 4.2 and 4.3.

To compare the model and real data, the FM plots for synthetic seismicity in variants 5.1 and 5.2 and that for observed seismicity constructed from catalog NEIC-5 are given in Fig. 15. For the model plots in Fig. 15, the magnitude interval (in the domain of average values), where the plots are "linear enough", is extended, in comparison with the modification with constant depth, see Fig. 13. However, as before, the plots essentially differ from the real one. To reduce differences in slopes, it is necessary to increase the number of model events outside the domain of average magnitudes. Toward this end, additional series of numerical experiments are assumed to be performed. Studying the shape and slope of the model plots shows that, according to some features, the results obtained for different depths of blocks are preferable than the results obtained for the same depth of blocks, and vice versa, according to other features.

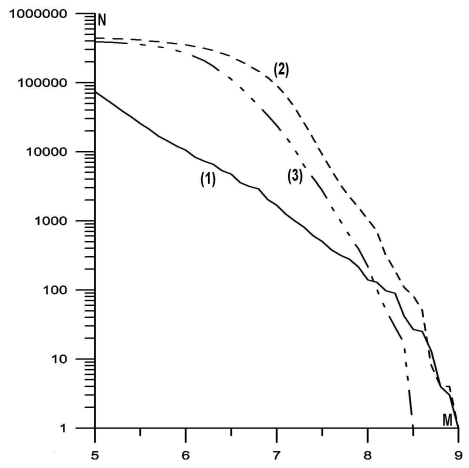

Figure 15: The FM plots constructed for the real (NEIC-5, (1)) and synthetic ((2) — variant 5.1, (3) — variant 5.2) catalogs; N is accumulated number of earthquakes, M is magnitude.

An additional comparative analysis of the two modifications of the spherical block model is carried out for the purpose of establishing the relation between model (dimensionless) and real time intervals. Relative velocities of displacements of characteristic points at plate boundaries obtained in the model are studied and compared with those given by the model HS2-Nuvel-1 [4]. The results are presented in Tab. 4.

Taking into account the quantitative behavior of displacements of points, we conclude that with rather high probability, for the dimensions accepted in the model, the unit of dimensionless model time corresponds to about 1 year for both variants. It is clear that this conjecture requires careful verification, first, by further comparative analysis of real and model catalogs, and second, by study of the impact of model parameters on the period between strong events in different regions. In addition, from Tab. 4 it follows that the velocities of relative displacements of boundary points in the modification with constant depth is more close to the HS2-Nuvel-1 velocities than in the modification with varying depth. The deviations are particularly large on the boundaries of the plates with greatly different values of depth (Cocos/Caribbean, Eurasia/Philippines). Note that in our experiment we consider the points on the Earth's surface, not at block bottoms, where one should expect less deviations from the HS2-Nuvel-1 velocities.

T a b l e 4

Velocities of relative displacements of boundary points:

(1) — in the model of plate motion HS2-Nuvel-1 (cm/year);

(2) — in the modification with constant depth (variant 3.4, Tab. 2, cm/unit of model time);

(3) — in the modification with varying depth (variant 5.1, Tab. 3, cm/unit of model time)

Point coordinates		Block		$\tan\alpha_1$	$\tan\alpha_2$	$\tan\alpha_3$	$\lvert\vec{v}_1\rvert$	$\lvert\vec{v}_2\rvert$	$\lvert\vec{v}_3\rvert$
latitude	longitude	I	II						
-21.71	-71.44	SA	N	0.23	0.22	0.24	8.66	8.06	8.15
-9.63	-13.25	SA	Af	0.22	0.20	0.21	3.28	3.36	3.45
11.19	-89.11	Ca	Co	1.89	1.69	1.54	7.95	7.10	12.16
-18.58	-112.63	P	N	-0.23	-0.23	-0.22	14.68	15.24	15.03
14.18	52.60	S	Ar	3.23	2.94	2.38	1.89	1.70	1.89
28.11	84.84	E	I	4.17	4.17	3.57	5.04	4.78	4.74
-49.85	130.44	An	Au	8.33	9.09	7.69	7.31	7.13	6.96
-7.00	149.62	P	Au	0.32	0.32	0.30	10.65	10.50	10.24
29.15	130.59	E	Ph	-0.80	-0.76	-0.06	5.12	5.17	3.99
36.89	-119.87	NA	P	-1.43	-1.41	-1.56	4.68	4.61	4.52

Remark. All the points considered belong to the Earth's surface. The coordinate system, in which relative displacements of a boundary point are considered, is connected with this point (the center is in the point, the axis x is directed along the parallel to the east, the axis y is directed along the meridian to the north). The fault segment that the point belongs to separates the blocks I and II, at that the block I is considered as motionless, whereas the block II moves relative to the block I. The vector of relative velocity $\vec{v}_i$ $(i = 1, 2, 3)$ is characterized by its absolute value $|\vec{v}_i|$ and the tangent of the angle α_i between $\vec{v}_i$ and the axis x.

The spatial distribution of the strongest model events in variant 5.1 (Fig. 16), being slightly different from the distributions obtained earlier (Figs. 11 and 14), nevertheless reveals an additional similarity with observed seismicity (Fig. 10), consisting in the occurrence of strong events on the north boundary India/Eurasia. It should be noted that the improvement of the model distribution takes place not due to matching faults parameters (which are the same for all experiments, see Tab. 1) but as a consequence of the development of the model.

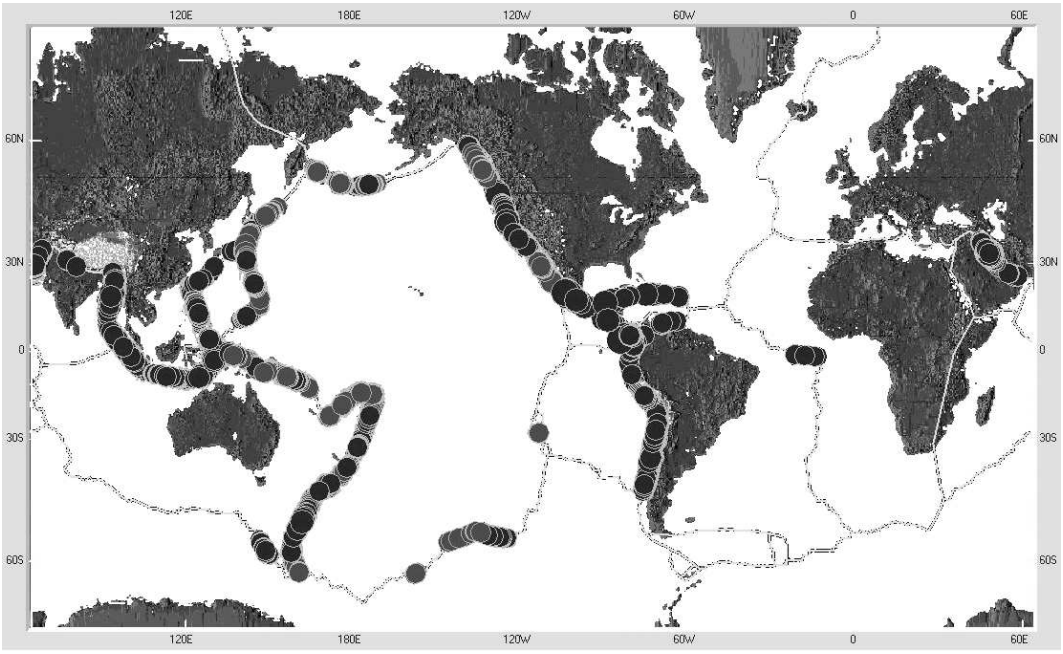

Figure 16: Epicenters of strongest earthquakes with $M \geq 7.0$, modification with varying depth, variant 5.1 from Tab. 3.

As to the spatial distribution of model events, note that, in the best variants for all the modifications, the most important patterns of global seismicity are reflected, namely: a) two large seismic belts, the circum-Pacific and Alpine-Himalayan (the first is more well-defined), where most of the strong earthquakes occur; b) extensive, but less pronounced seismicity at mid-oceanic ridges; c) increased seismic activity associated with triple junctions of plate boundaries. At the same time, the absence of earthquakes in oceanic rift zones in the model is related to parameter fitting. At the current stage of investigations, an intensive quantitative study of the real and model distributions seems to be possible, but not productive because firstly, observed seismicity is rather weak on many parts of plate boundaries (due to the relative smallness of the observation interval), and secondly, the range of model magnitudes is too narrow and does not correspond to the real one. To find adequate correspondence between model and real magnitudes is the subject of a separate investigation, because this correspondence may be different in different seismic regions.

Among experiments that are specific for the last modification of the model, we point out here the analysis of the distribution of model events with respect to depth. Note that a "good" similarity of the model distribution with the real one would allow us to pass to studying the migration of model events and the mechanism of their spreading along a fault.

The results for characteristic depths of the model structure are given in Tab. 5. It is evident that, in order to redistribute events, we need to get more specific information on the rule of changing model parameters depending on depth. We observe the noticeable similarity between the real distribution and results obtained in variant 5.1, where changes concern the values describing the interaction of blocks and underlying medium.

T a b l e 5

Distribution of earthquakes with respect to depth (in percent with respect to the total number of events with magnitude not less than 5.0): NEIC — global catalog NEIC-5 (73 891 events); 4.1 — variant 4.1 (494 449); 4.2 — variant 4.2 (556 018); 4.3 — variant 4.3 (780 006); 5.1 — variant 5.1 (445 248); 5.2 — variant 5.2 (392 477)

Depth	NEIC	4.1	4.2	4.3	5.1	5.2
up to 30 km	35.3	46.4	65.1	31.2	40.9	46.5
[30, 50 km]	32.6	29.4	29.4	20.9	31.6	31.0
over 50 km	32.1	24.2	5.5	47.9	27.5	22.5

4 Parallelization: key aspects and efficiency

The computational experiments described in the previous sections show that the spherical block model of lithosphere dynamics and seismicity during performing on sequential computers requires very considerable expenditures of memory and processor time. Due to this reason, the problem of simulating dynamics for structures with a large number of blocks and small enough steps of the temporal-spatial discretization needs special solving tools. Note that considering the spherical geometry of the structure essentially complicates calculations and introducing depth in the model (implying the discretization of segments by depth) is a real technical problem (because faults are cone surfaces). However, the approach applied to modeling admits effective parallelization of calculations on a multiprocessor machine [10, 18]. The standard scheme "master-worker" ("processor farm") is engaged. For compatibility with different platforms (in the sense of fast transition), the special library MPI ("Message Passing Interface") is used, and the parallel algorithm is designed in such a way that a unique loading module is formed for all processors.

The flowchart of the main calculative procedure is presented in Fig. 17. Let us give necessary explanations.

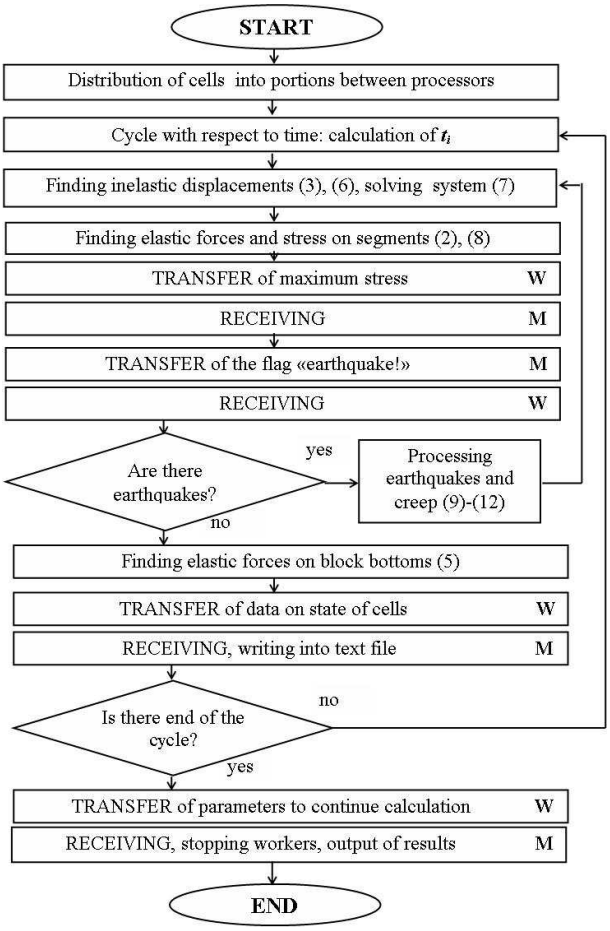

Figure 17: Flowchart of main calculative procedure.

In the beginning of the work, a specific processor, which the program has loaded to, is detected by its number (zero number becomes the master). Then the information on the block structure is read, and auxiliary calculations (the space discretization, calculation of the matrix $\mathbf{A}$ of system (7)) are performed. For all the modifications of the model, at every time step, the most time-consumable procedure is calculation of the values of forces and inelastic displacements in all cells of the space discretization of the block bottoms and fault segments. Since these calculations can be performed independently from each other, it is necessary to share them uniformly between all processors. Note that, calculating all the values above at its own portion of cells, the master plays the role of the worker as well. Namely the uniform distribution of cells and organizing the optimal informational exchange between processors are key elements of the parallel algorithm in question. Let us stop on these aspects in more detail.

In the problem considered, the natural way of organizing data associated with fault segments (these data (coordinates of cells, forces, and displacements) require a major part

of the memory) is the usage of two-dimensional arrays of the form f_{ij}, where i is the number of the cell of the surface discretization of the segment in the global numeration of all surface cells through all segments of the structure, j is the number of the vertical layer of the discretization of the segment by depth. Note that such a way of data storage provides data compatibility for all the modifications of the model (without and with depth). The distribution of segment cells between processors is performed without crippling the layers, as shown in Fig. 18.

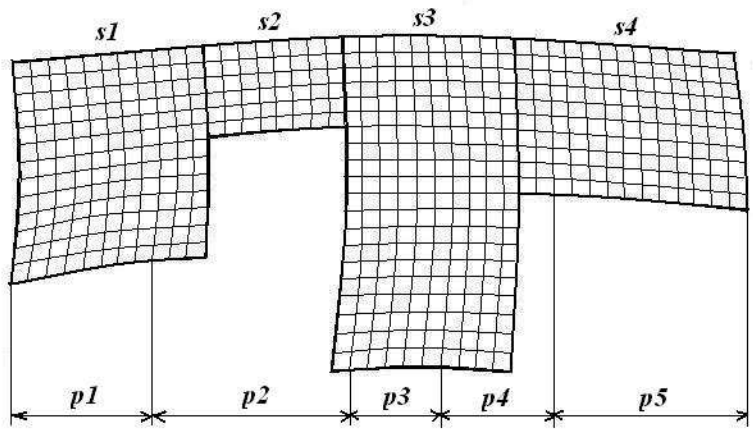

Figure 18: Example of distribution of segment cells: four segments (s1-s4), five processors (p1-p5).

The dynamical allocation of the memory for a two-dimensional array on each processor is implemented by means of the memory allocation for the array (its length is equal to the number of surface cells distributed to this processor) of pointers to the one-dimensional arrays of variable length corresponding to the layers of the discretization by depth:

```
f_l=(double**)calloc(cells[n_pr],sizeof(double*))
```

Here `f_l` is the two-dimensional array, `n_pr` is the processor number, `cells[n_pr]` is the number of surface cells on processor `n_pr`. Further, the memory for the one-dimensional arrays is allocated:

```
f_l[0]=(double*)calloc(ncells[n_pr],sizeof(double));


for(i=1;i<cells[n_pr];i++) {f_l[i]=f_l[i-1]+n[i-1];}
```

Here `ncells[n_pr]` is the total number of cells of the array `f_l` distributed to the processor `n_pr`, `n[i-1]` is the depth of the layer corresponding to the cell `i-1`.

The exchange of information is realized according to the following scheme (see Fig. 17, where the operations carried out only by the master are marked by "M", only by the workers – by "W", both by the master and the workers are not marked). At every time step, the master calculates new values of block, boundary block, and underlying medium displacements (it requires insignificant time due to the small dimension of system (7)), then necessary parameters are transferred to the workers. Recalculated values of the forces, the inelastic displacements, and the vector $\mathbf{b}$ are returned to the master, then the next time step is carried out. For processing the situation treated as an earthquake, the scheme is slightly complicated, since in this case the master should ask all the workers until cells of segments in the critical state exist (for which $\kappa \geq B$); then the master receives the information on model events and writes it into a file of special structure. For such a scheme, the time of calculations on each processor is much more than the time of exchange. Therefore, rather high useful loading of each processor is achieved.

The simulation was performed at the Joint Supercomputer Center (Moscow, Russia; Supercomputer MVS-1000K, 990 CPUs 2×4 core Intel Xeon (3 GHz), the peak performance is about 95 TFlops) and at the Institute of Mathematics and Mechanics (Ekaterinburg, Russia; UM64 machine, 108 processors Opteron (2.6 GHz), the peak performance is about 560 GFlops). In addition, on UM64 machine, the experiments for testing the dependence of time necessary for solving the problem on the number of processors were carried out. A time-taking variant with a considerable number of earthquakes occurred was chosen; 100 time steps were considered (note that a typical variant needs 20 000 steps). The speedup, the granularity level, and the efficiency were analyzed. The results of testing are presented in Tab. 6. It should be noted that both T_1 and T_p essentially depend on parameters of the structure under consideration but for all variants their ratio is approximately the same.

T a b l e 6

Dependence of speedup and efficiency on the number of processors

p	t_{calc}	t_{exch}	t_{tot}	S_p	E_p^1	G	E_p^2
1	6335.84	–	6335.84	–	–	–	–
2	3256.52	34.60	3291.12	1.92	0.96	94.12	0.99
4	1626.94	38.52	1665.46	3.80	0.95	42.24	0.98
8	814.74	33.98	848.72	7.46	0.93	23.98	0.96
10	654.34	27.93	682.27	9.29	0.93	23.43	0.96
16	417.36	22.26	439.62	14.41	0.90	18.75	0.95
20	331.23	22.33	353.56	17.92	0.90	14.83	0.94
28	237.08	28.53	264.61	23.94	0.86	8.31	0.89

Notation: p is the number of processors, t_{calc} is calculation time, t_{exch} is idle and exchange time, t_{tot} is total expenditure time (all in seconds), $S_p = T_1/T_p$ is speedup, T_1 is performance time for sequential algorithm, T_p is performance time for parallel algorithm on p processors, $G = t_{\text{calc}}/t_{\text{exch}}$ is granularity level, $E_p^1 = S_p/p$, $E_p^2 = G/(G+1) = t_{\text{calc}}/t_{\text{tot}}$ are efficiencies (the last one is also called processor utilization).

It follows from Tab. 6 that for $p \leq 20$ the speedup S_p is slightly less than p, the efficiencies E_p^1 and E_p^2 are rather high, not less than 0.9. The value E_p^2, which is calculated without executing the sequential algorithm, appropriately approximates E_p^1; this is in agreement with theoretical results. It is important that, after introducing the spherical geometry, the volume of calculations essentially increases, whereas exchanges between processors remain almost the same. Therefore, the share of calculation time (in the total time) increases with respect to the share of idle and exchange time; this results in the efficiency increase comparing with the modification without depth.

5 Conclusive remarks

Simplifications accepted in the spherical block-and-fault model give no opportunity to draw conclusions on the correspondence between observed and synthetic seismicity at any specific point or in relatively small regions. However, some similarity of the model results and the real data in the global scale is certainly a positive fact; it stimulates a further development of the model.

Basing on the results of numerical experiments, we established that, according to some characteristics, the modifications with depth are more adequate in the description of dynamics and seismicity of the global system of tectonic plates than the modification without depth. It should be noted that this happens despite the fact that the depth is significantly less than the linear dimensions of plates and, seemingly, may be neglected when simulating. The matter is that, in the case of the modification without depth, the role of dip angles of faults is leveled, whereas these angles play a determinative role in properties of synthetic seismicity. However, the modification without depth may be used for the qualitative studying of the interaction between blocks along their boundaries and such properties of a seismic flow as the spatial distribution of epicenters, the seismic cycle, and the migration of events along tectonic faults. Its main advantage consists in considerable saving of running time during simulations; the cons are obvious. The modification with constant depth allows us to start studying the mechanism of spreading earthquakes along a fault, to classify events, and to essentially extend the range of changing the model magnitude. The recently developed modification, the modification with varying depth, being an attempt of taking into account the lithosphere inhomogeneities within the framework of the spherical block model, opens additive possibilities in simulation, in particular, provides an opportunity of investigating distributions of model events with respect to depth and studying the dependence of synthetic seismicity on different rules of changing visco-elastic properties of a fault medium with depth.

Acknowledgements

This work has been partly done at the Abdus Salam International Center for Theoretical Physics (Trieste, Italy). It was performed within the framework of the Program of Presidium of Russian Academy of Sciences "Intellectual information technologies, mathematical modeling, system analysis, and automatization" and for the first author was supported by the Russian Foundation for Basic Research (Project 09-01-00378) and also by the Ural-Siberian Interdisciplinary Project. The authors are thankful to Prof. Alik Ismail-Zadeh for fruitful discussion and advice.

References

[1] **Gabrielov A. M., Keilis-Borok V. I., Levshina T. A., and Shaposhnikov V. A.**

Block model of lithosphere dynamics // Computational Seismology, Vol. 19. Moscow, Nauka, 1986. P. 168–178.

[2] **Gabrielov A. M., Newman W. I.** Seismicity modeling and earthquake prediction: a review // Geophysical Monograph 83. IUGG, 1994. Vol. 18. P. 7–13.

[3] **Global hypocenters data base CD-ROM** // NEIC/USGS, Denver, CO, 2009.

[4] **Gripp A. E., Gordon R. G.** Young tracks of hotspots and current plate velocities // Geophys. J. Int. 2002. Vol. 150. P. 321–361.

[5] **Ismail-Zadeh A. T., Le Mouel J.-L., Soloviev A. A., Tapponnier P., and Vorobieva I. A.** Numerical modeling of crustal block-and-fault dynamics, earthquakes and slip rates in the Tibet-Himalayan region // Earth and Planetary Science Letters, 2007, Vol. 258. P. 465–485.

[6] **Jestin F. P., Huchon P. J., and Gaulier M.** The Somalia plate and the East African rift system: present-day kinematics // Geoph. J. Int. 1994. No. 116. P. 637–654.

[7] **Keilis-Borok V. I., Rotwain I. M., and Soloviev A. A.** Numerical modelling of block structure dynamics: dependence of a synthetic earthquake flow on the structure separateness and boundary movements // J. of Seismology, 1997. No. 1. P. 151–160.

[8] **McKnight T.** Geographica: The complete illustrated Atlas of the world. New York: Barnes and Noble Books, 2004.

[9] **Melnikova L. A., Rozenberg V. L., Sobolev P. O., and Soloviev A. A.** Numerical simulation of dynamics of a system of tectonic plates: spherical block model // Computational Seismology, Vol. 31. Moscow, GEOS, 2000. P. 138–153.

[10] **Melnikova L. A., Rozenberg V. L.** Spherical block model of lithosphere dynamics and seismicity: different modifications and numerical experiments // Proceedings of IMM UB RAS, Vol. 13 (3). Ekaterinburg, 2007. P. 95–120.

[11] **Mutter J. C.** Seismic images of plate boundaries // Scientific American, 1986. Vol. 254. P. 66–75.

[12] **Panza G. F., Soloviev A. A., and Vorobieva I. A.** Numerical modelling of block-structure dynamics: applications to the Vrancea region // Pure Appl. Geophys. 1997. No. 149. P. 313–336.

[13] **Rozenberg V. L., Soloviev A. A.** Considering 3D movements of blocks in the model of block structure dynamics // 4th Workshop on Non-Linear Dynamics and Earthquake Prediction. Trieste: Italy. 6–24 October, 1997. Preprint, SMR.1011-3.

[14] **Rozenberg V. L., Sobolev P. O., Soloviev A. A., and Melnikova L. A.** The spherical block model: dynamics of the global system of tectonic plates and seismicity // Pure Appl. Geophys. 2005. No. 162. P. 145–164.

[15] **Rozenberg V. L., Melnikova L. A., and Soloviev A. A.** The spherical block model: application of different modifications to modeling dynamics and seismicity of the global system of tectonic plates // 9th Workshop on Non-Linear Dynamics and Earthquake Prediction. Trieste: Italy. 1–13 October, 2007. Preprint, SMR.1864-20.

[16] **Rundquist D. V., Soloviev A. A.** Numerical modeling of block structure dynamics: an arc subduction zone // Phys. Earth Planet. Int. 1999. Vol. 111, No. 3. P. 241–252.

[17] **Sobolev P. O., Soloviev A. A., and Rotwain I. M.** Modeling of lithosphere dynamics and seismicity for the Near East // Computational Seismology and Geodynamics. Ed. Chowdhury D. K. American Geophysical Union, Washington, D.C., 1999. Vol. 4. P. 115–123.

[18] **Soloviev A. A., Maksimov V. I., Rozenberg V. L., and Ermoliev Y. M.** Block models of lithosphere dynamics: approach and algorithms // Lecture Notes in Computer Science 2328, Volume on Parallel Processing and Applied Mathematics. Springer, 2001. P. 572–579.

[19] **Soloviev A. A., Ismail-Zadeh A. T.** Models of dynamics of block-and-fault systems // Nonlinear Dynamics of the Lithosphere and Earthquake Prediction. Ed. Keilis-Borok V. I., Soloviev A. A. Springer, 2003. P. 71–139.

[20] **Utsu T., Seki A.** A relation between the area of aftershock region and the energy of main shock // J. Seism. Soc. Japan, 1954. Vol. 7. P. 233–240.

[21] **Wells D. L., Coppersmith K. L.** New empirical relationships among magnitude, rupture length, rupture width, rupture area, and surface displacement // Bull. Seism. Soc. of America, 1994, Vol. 84, No. 4. P. 974–1002.